SUPPLEMENTAL MATERIAL

Supplemental Methods

Plasmid constructs. A description of relevant plasmids and viruses is provided below. Additional details for all constructions are available upon request. Many of these plasmids were constructed by Genewiz using the methods of the company's choice. All AAV were produced by the University of Pennsylvania Vector Core with funding provided in part by the NHLBI Gene Therapy Resource Program.

Adenoviruses were prepared using the pTRE shuttle vector and the Adeno-X Tet-off System (Clontech) via PI-Sce I and I-Ceu I subcloning and purified after amplification using Vivapure AdenoPACK kits (Sartorius Stedim). These adenovirus conditionally express recombinant protein when co-infected with tetracycline transactivator-expressing virus (adeno-tTA for "tet-off" or reverse tTA for "tet-on"). Some adenoviruses were constructed using a modified pTRE shuttle vector (pS) containing the constitutive CMV immediate early promoter or a modified pTRE shuttle vector containing a U6 promoter for expressing shRNA.[40]

The myc-tagged human CIP4h expression vector pCM-CIP4h was as previously described.[25] The yeast-two hybrid PP bait vector was constructed by inserting oligonucleotides with XmaI - SalI overhangs encoding mouse CaNAβ 1-27 into pLEXNA.[41] HA-tagged CaNA rat α and mouse β2 subunit pTRE expression vectors were as previously described.[42] pTRE-HA-CaNAβ2 H160Q was generated by site-directed mutagenesis using the expression plasmid for wildtype CaNAβ2 replacing GAGAGGCAACCAT with CCGCGGCAACCAA. pTRE-HA-CaNAβ2 ΔPP was constructed by deletion of the codons for CaNAβ aa 3-23 in pTRE-HA-CaNAβ. pTRE-

HA-CaNAβ2 ΔPP H160Q was constructed by subcloning the MscI – BsrGI fragment of pTRE-HA-CaNAβ2 H160Q into pTRE-HA-CaNAβ2 ΔPP. pTRE-HA-CaNAα H151Q was generated by mutagenesis of pTRE-HA-CaNAα replacing TGAATGT with AGAATGC. pTRE-HA-CaNAα+PP was constructed by replacing the SacII – AccI cDNA fragment in pTRE-HA-CaNAα encoding the HA tag and CaNAα 1-11 with the comparable fragment from pTRE-HA-CaNAβ2 encoding the HA tag and CaNAβ 1-23.

The CaNAβ PP-GFP adenovirus was constructed by first inserting oligonucleotides with EcoRI - SalI overhangs encoding mouse CaNAβ 1-24 into pEGFPN3 (Clontech), followed by cDNA subcloning into pTRE and Adeno-X. The CaNAβ PP-BFP adenovirus was constructed by subcloning the EBFP cDNA from pEBFP2-nuc (a gift from Robert Campbell - Addgene plasmid #14893)[43] 3' to a cDNA fragment encoding CaNAβ 1-25 in the pS shuttle vector. pAcTNT-EGFP-mh for producing AAV9.GFP was constructed by inserting a myc-His_6 C-terminally tagged EGFP cDNA into the NheI and BamHI sites of pAcTnTs containing the chicken cardiac troponin T promoter and flanking AAV2 inverted terminal repeats generously provided by Dr. Brent French.[18] pAcTnT-CaNAβ PP-EGFP-mh for producing AAV9.PP-GFP was constructed by inserting a synthetic sequence encoding mouse CaNAβ 1-27 into the NheI and NcoI sites in pAcTNT-EGFP-mh.

Rat shRNA adenoviral shuttle vectors were as previously described for the control shRNA.[40] and contained the following shRNA sequences: CaNAα.[44] - CAAGATCCGAGCAATAGGCTTCAAGAGAGCCTATTGCTCGGATCTTGTTTTTT; CaNAβ2 - TTTAAGACCATGCTAATCCTTCAAGAGAGGATTAGCATGGTCTTAAA.

The NFATc1-based EGFP-mCherry FRET sensor CaNAR-CIP4 was similar in design to the NFATc2-based ECFP-Venus calcineurin activity reporter published by the Zhang laboratory,[45] that shows increased FRET signal when dephosphorylated by calcineurin. The NFATc1 regulatory domain was included instead of that from NFATc2, since NFATc1 is activated by more diverse stimuli than NFATc2 in myocytes.[46] Accordingly, the expression plasmid pS-CaNAR-CIP4 was constructed so as to insert into pS adenovirus shuttle vector a cDNA encoding the following fusion protein: mCherry - human NFATc1 aa 2-311 (Genbank NM_172390 bp 457-1386) - EGFP - myc tag - human CIP4h. The cytosolic CaNAR expression vector was generated by deleting a HpaI - SrfI fragment in pS-CaNAR-CIP4, leaving the myc tag, but deleting the CIP4h open reading frame. pmCherry-NFAT-EGFP, a plasmid encoding the same parent sensor without a myc tag and not adenovirus compatible, was also used for initial characterization.

The ECFP-cpVenus FRET sensor D3cpv Cameleon was a gift from Amy Palmer & Roger Tsien (Addgene plasmid # 36323).[39] Adenovirus to express Cameleon were generated by insertion of the Cameleon cDNA into the pS shuttle vector. Adenovirus to express Cameleon-CIP4 were generated by insertion of the Cameleon cDNA via PCR cloning into the SacII and NcoI sites of a pTRE-myc-CIP4 shuttle vector.

Antibodies.

Antigen	*Species and Catalog number*	*Company*
α-actinin	mouse monoclonal EA-53	Sigma-Aldrich
CaNAβ2	rabbit 07-068	Millipore
CaNAα	rabbit 07-067	Millipore
CIP4	mouse H00009322-M01	Abnova
CIP4	rabbit OR049	Kapiloff lab.[25]

GFP	Rabbit sc-8334	Santa Cruz
Flag tag	Rabbit F7425	Sigmal-Aldrich
HA tag	Mouse HA-7 monoclonal	Sigma-Aldrich
Myc tag	Mouse 4A6 monoclonal	Millipore
Myc tag	rabbit 06-549	Millipore

Yeast 2-Hybrid. A pACT2-based human heart yeast two-hybrid library (Clontech) was screened with a pLexNA bait vector that expresses the N-terminal 27 residues of CaNAβ in fusion to LexA with a nuclear localization signal (Figure IB in Data Supplement), using published protocols.[41] In brief, following prior transformation with the pLEXNA-CaNAβ PP bait plasmid, the pACT2 library was transformed into the L40 MATa yeast strain containing LYS2::(lexAop)4-HIS3 and URA3::(lexAop)8-lacZ cassettes. Clones were selected for *HIS3* gene complementation (histidine production) on agar plates lacking histidine, tryptophan (provided by pLEXNA), leucine (provided by pACT2), lysine, and uracil. β-galactosidase activity assay was used as a secondary assay. Of 1.5 million original transformants, 52 clones survived selection and were analyzed further by loss of the bait plasmid and mating to AMR70 MATα yeast previously transformed with pLEXNA bait plasmid or a negative control pLEXNA plasmid containing an AKAP18 cDNA. Of these, 31 pACT2 clone plasmids were transformed into bacteria and analyzed by DNA sequencing.

Animal Models. All *in vivo* research was performed under the supervision of the Institutional Animal Care and Use Committee at the University of Miami. All rats used in this project were Sprague-Dawley, and all mice used in this project were C57BL/6. The conditional “floxed” *CIP4* (*TRIP10*) mouse designed to delete *CIP4* exons 2 and 3 and introduce a frameshift in exon 4 was generated by the University of Cincinnati Gene

Targeted Mouse Service Core by ES cell line homologous recombination and blastocyst injection (Supplementary Fig. 2A). After mating to a Flp recombinase transgenic mouse, *CIP4*$^{f/+}$ mice were mated to either B6.C-Tg(CMV-cre)1Cng/j (strain 006054) or B6.FVB(129)-*A1cf*$^{Tg(Myh6\text{-}cre/Esr1*)1Jmk}$/J (strain 005657)[12] mice (The Jackson Laboratory) to provide constitutive global and tamoxifen inducible, cardiac myocyte-specific gene deletion, respectively. Genotype was determined by PCR analysis of DNA extracted from tail or ear tissue. *Cre* transgenes were detected using primers TGGATAGTTTTTACTGCCAGACCGCGC and TGACCGTACACCAAAATTTGCCTGCA. *CIP4* alleles were differentiated using the following primers: P1 - CTGAGTCACTCAACTGAGGATC, P2 - CAGGCACAGAAGGGATGAGTTC, P3 - TGCACCCACTTATCCACAGAAC, and P4 - TGGCTAAAGGGAGTAACAGGAC. After Flp recombination, PCR results were as follows: P1-P2: WT - 120 bp, Floxed - 164 bp; P3-P4: WT - 204 bp, Floxed - 332 bp; P1-P4 - KO - 337 bp. To induce gene knock-out, 8 week old *CIP4*$^{f/f}$;Tg(Myh6-cre/Esr1*) "CIP4 CKO" mice were fed tamoxifen-laden chow (125 mg tamoxifen/kg chow, Harlan Teklad) for 1 week before restoration of normal chow for 1 week before use in experimentation. All control Tg(Myh6-cre/Esr1*) "MCM" and *CIP4*$^{f/f}$ mice were similarly treated with tamoxifen before study. For AAV studies, 2-3 day old wildtype mice were injected intraperitoneally with 10^{11} GC AAV in 20 µl saline.

For all *in vivo* studies, both male and female mice were used. Masking of cohorts was provided by assigning a random number to each mouse by ear tag, after genotyping in the case of CIP4 CKO and control mice, such that identification of mouse cohort was not revealed until *in vivo* and post-mortem analyses were complete. A formal

power analysis was not performed for the exploratory studies in this project, albeit the numbers of mice used were in excess of those typically necessary for pressure overload studies to allow for tissue collection for use in ancillary biochemical and histological studies.

Transverse Aortic Constriction. To induce cardiac pressure overload, mice aged 8 to 10 weeks were subjected to TAC survival surgery, as previously described.[16] In brief, the transverse aortic arch was visualized after midline sternotomy, and a silk ligature (6-0) was passed around the aorta between the brachiocephalic and left common carotid arteries. A 27 gauge needle was placed on top of the aorta, and the 6-0 silk tied around the needle. The needle was removed, and the chest was closed. Sham-operated mice without the placement of the aortic ligature served as controls. Only mice with a carotid artery flow ratio of 5-12 were included in the studies. For long-term TAC survival studies, mice in extremis were euthanized and counted as mortality events, i.e., mice that exhibited minimal movement, a moribund respiratory pattern and/or severe tachypnea, or acute severe edema.

Echocardiography. Mice minimally anesthetized with 0.5-2% isoflurane were studied by transthoracic echocardiography using a Vevo 770® or Vevo® 2100, High-Resolution Imaging System (VisualSonics) as previously described.[16] Using B-mode parasternal short-axis LV images for orientation, M-mode images at level of the papillary muscles level were obtained. To determine extent of aortic constriction in mice subjected to pressure overload, blood flow velocities in the right and left carotid arteries were

recorded by Doppler imaging, and the ratio of right to left carotid artery flow determined. Calculated parameters from at least three cardiac cycles by M-mode echocardiographs were as follows: FS, fractional shortening = (LVID;d – LVID;s)/(LVID;d); EF, ejection fraction = (LVV;d – LVV;s)/(LVV;d), in which LVV (in μL) = $LVID^3$ * 7/(2.4 + LVID) for either systole or diastole; LV Mass (in mg) = $0.84((LVID;d + LVPW;d + LVAW;d)^3 – LVID;d^3)$. Data were calculated using VevoLAB software (Visualsonics).

Histology. Mouse heart tissues were fixed with 10% formalin, embedded in paraffin, and microtome sectioned at 5 μm thickness. After deparaffinization, sections were stained with Masson Trichrome Kit (Thermo Fisher Scientific), Alexa Fluor 555 conjugated Wheat Germ Agglutinin (Invitrogen), Picrosirius Red Stain Kit (Polysciences), and *In Situ* Cell Death Detection Kit, TMR red (Roche), according to the manufacturer's instructions/protocols. Images were acquired using a widefield Leica DM4000 B LED microscope and IPLab image software (BD Biosciences). The cross-section area of myocytes in transverse section was determined using the wheat germ agglutinin-stained sections, >200 myocytes in >3 distinct fields per mouse. Myocardial fibrosis was assayed by determining the fraction of LV area representing picrosirius red-stained collagen fibers using circularly polarized light microscopy to image entire LV sections. TUNEL staining counterstained with DAPI was fluorescently imaged to determine myocardial cell death.

Adult rat ventricular myocyte isolation and culture: 2-3 months old rats were anesthetized using Ketamine (80-100 mg/kg) and Xylazine (5-10 mg/kg) IP following

1000 U heparinization for cardiac excision. The heart was transferred immediately into chilled perfusion buffer (NaCl 120 mmol/L, KCl 5.4 mmol/L, $Na_2HPO4 \cdot 7H_2O$ 1.2 mmol/L, $NaHCO_3$ 20 mmol/L, $MgCl_2$.6H2O 1.6 mmol/L, Taurine 5 mmol/L, Glucose 5.6 mmol/L, 2,3-Butanedione monoxime 10 mmol/L) pre-equilibrated with 95% O_2 and 5% CO_2. After removal of extraneous tissue, the heart was attached via the aorta to a Harvard Langendorff apparatus cannula. Ca^{2+}-free perfusion was used to flush out remaining blood with a constant rate of 8-10 mL/min at 37ºC. The heart was then digested through circulatory perfusion with 50 mL perfusion buffer containing 125 mg type II collagenase (Worthington, 245U/mg), 0.1 mg protease (Sigma type XIV) and 0.1% BSA. After perfusion, the atria were removed and the ventricular myocytes dissociated by slicing and repetitive pipetting. The debris was filtered by a 150 - 200 μm nylon mesh, and the myocytes collected by one minute centrifugation at 50 x*g*. Ca^{2+} concentration in the buffer was gradually increased to 1.8 mmol/L and the myocytes were resuspended in ACCT medium (M199 Medium [Invitrogen 11150-059], Creatine 5 mmol/L, L-carnitine 2 mmol/L, Taurine 5 mmol/L, HEPES 25 mmol/L, 2,3-Butanedione monoxime 10 mmol/L, BSA 0.2% and 1X Insulin-Transferrin-Selenium Supplement) and plated on 10 μg/ml laminin pre-coated dishes. Cells were washed with ACCT medium 1.5 hours after plating and subjected to adenoviral infection. Adrenergic agonists were added on the 2nd day in culture, with immunocytochemistry performed after 24 hours of stimulation as previously described.[13] At least 50 myocytes were measured for length and width for each experimental replicate in the morphologic studies by widefield microscopy using IPLab microscope software (BD Biosciences) or Leica LAS software.

Other Cell Culture. HEK293, HeLa and COS-7 cells were maintained in DMEM with 10% FBS and 1% P/S. These cells were transiently transfected with Lipofectamine 2000 (Invitrogen) or JetPEI (Polyplus) or infected with adenovirus and Adeno-X Tet-Off virus (Clontech) as suggested by the manufacturers. Neonatal rat ventricular myocytes were prepared as previously described.[13]

FRET Imaging. Adult rat ventricular myocytes were isolated as described above, plated on laminin-coated glass coverslips and infected with adenoviruses encoding a FRET sensor with and without HA-CaNA and tTA and/or CaNA shRNA viruses, as indicated, all at multiplicity of infection 300. 2,3-Butanedione monoxime was not included in the medium in order to allow for comparison of paced beating cells with those neurohormonally stimulated. 2 days after viral transduction, cells were washed with buffer (20 mmol/L glucose, 135 mmol/L NaCl, 4.7 mmol/L KCl, 0.6 mmol/L Na_2HPO_4, 0.6 mmol/L KH_2PO_4, 1.2 mmol/L $MgSO_4$, 1.5 mmol/L $CaCl_2$ and 10 mmol/L HEPES, pH 7.4) and stimulated in the same buffer with 1 hz pacing or hypertrophic agonist while monitoring FRET. FRET imaging was performed using a custom imaging system, consisting of 440nm (Cameleon) and 490 nm (CaNAR) pE-100 light emitting diodes (CoolLED) to excite the biosensors, a Leica DMI3000 microscope equipped with a 63x oil immersion objective, and a DV2 DualView beam splitter (Photometrics). For CaNAR imaging, there was a 490/30 ET excitation filter, and the DualView was equipped with a 565dcxr dichroic mirror, D520/30 and D630/50 emission filters. For Cameleon imaging there was a 436/30 ET excitation filter, 455 LP dichroic in the microscope cube, and 505dcxr dichroic mirror, 480/30 and 535/40 ET emission filters in the DualView.

Fluorescence for the individual channels was recorded with a OptiMOS camera (Photometrics) using the open source MicroManager 1.4 software.[47] FRET ratios (R = $FRET_c$ ÷ Donor), where $Fret_c$ is FRET signal corrected for the bleedthrough of the donor into the acceptor channel, was analyzed using Origin 8.0 software as described.[48] Representative FRET tracings showing normalized FRET ratios (R/R_0) are shown after 2nd order and 5 neighbor smoothing (Graphpad Prism 8). Percent change in FRET ratios from baseline to plateau ($\Delta R/R_0$ x100) are presented graphically and represent tracings from at least 3 different myocyte preparations. HeLa cells were imaged similarly following stimulation with 10 μM Ca^{2+} ionophore A23187 (Sigma).

Immunoblotting. Flash-frozen tissue was homogenized in buffer (20 mmol/L HEPES, pH 7.4, 150 mmol/L NaCl, 5 mmol/L EDTA, 0.5% Triton, 50 mmol/L NaF, 1 mmol/L sodium orthovanadate, 1 mmol/L DTT, and protease inhibitors) using a Polytron. Protein concentration was determined by Bio-Rad Protein Assay. The extracts were size-fractionated by SDS-PAGE. Protein markers were Precision Plus Protein Standards (Bio-Rad). Equal loading was confirmed by Ponceau S staining of blotted gels. Immunodetection was performed using primary antibodies and donkey anti-IgG-horseradish peroxidase antibody conjugates (Jackson immunoResearch) and imaging using Supersignal West Chemiluminescent Substrates (Thermo Scientific) and a LAS-3000 (Fujifilm) or an Amersham Imager 600 imaging system (GE Healthcare Life Sciences). Cultured cells were similarly lysed in buffer and analyzed by western blotting.

Co-Immunoprecipitation. For immunoprecipitation, cells were lysed in IP buffer (50 mmol/L HEPES pH 7.4, 150 mmol/L NaCl, 5 mmol/L EDTA, 10% glycerol, 1% Triton-X 100, 1 mmol/L DTT) plus an inhibitor cocktail (1 µg/ml leupeptin, 1 µg/ml pepstatin, 1 mmol/L benzamidine, 1 mmol/L AEBSF, 50 mmol/L NaF, 1 mmol/L sodium orthovanadate). Cleared lysates were incubated with antibody and 10 µl pre-washed protein-G agarose beads (50% slurry, Upstate) and incubated overnight with rocking at 4°C. Beads were washed four times for 5 minutes at 4°C with IP buffer. Bound proteins were size-fractionated on SDS-PAGE gels and developed by immunoblotting as described above.

Proximity Ligation Assay. PLA was performed using Duolink In Situ Kit (Sigma) or an equivalent in house prepared kit, as directed by the manufacturer. Briefly, adenovirus-infected rat myocytes or acutely isolated adult mouse ventricular myocytes plated on laminin-coated glass coverslips were fixed, permeabilized, and incubated with mouse anti-CIP4 or mouse IgG control antibodies and rabbit anti-CaNA antibodies. PLA signal was detected using “minus” mouse and “plus” rabbit oligonucleotide probes, followed by ligation of probes with circularization oligonucleotides, signal amplification by primer extension with Phi29 DNA polymerase, and detection using Alexa 555-conjugated detection oligonucleotide. PLA signal “events” were quantified by counting fluorescent spots on cells using a Leica DM4000 wide-field microscope (Fig. 3C) or following image flattening by maximum image projection of Airyscan processed Zeiss confocal microscopy images (Fig. 1C). The average number of spots in 10-20 myocytes was determined for each experimental replicate. While PLA may detect only a small fraction

of the cellular protein complexes of interest and confers low spatial resolution, it is an assay for endogenous protein-protein interactions (<40 nm distance) that is highly specific and does not require complex stability after cell lysis as during immunoprecipitation.[49] PLA images, however, are not reliable for intracellular localization.

Nanostring. Nanostring assay was used to determine mRNA levels for genes of interest and was performed at the Center for Genome Technology in the John P. Hussman Institute for Human Genomics at the University of Miami Miller School of Medicine. Total RNA was quantified with a Nanodrop 8000 Spectrophotometer (Thermo Scientific) and quality controlled using with a Bioanalyzer 2100 and the RNA 6000 Nano kit (Agilent). The NanoString assay is based on direct, multiplexed measurement of gene expression without amplification, utilizing fluorescent molecular barcodes and single molecule imaging to identify and count multiple transcripts in a single reaction. For Nanostring assay, 100 ng total RNA were hybridized in solution to a target-specific codeset overnight at 65˚C. The codeset contained dual, adjacently placed 50 bp oligonucleotide probes against a panel of genes, one set of probes fluorescently bar-coded and the other biotinylated. The hybridization reactions were loaded onto the NanoString Prep station which removes excess oligonucleotides and binds the hybridized mRNA to the Streptavidin-coated cartridge surface. The cartridges were loaded onto the NanoString Digital Analyzer, and 555 fields of view were fluorescently scanned to count only those individual mRNAs bound to both a biotinylated and fluorescently bar-coded probe. Datasets for each RNA sample were background-

subtracted and normalized using the housekeeping gene *Hprt* using nSolver 4 software. Probe sequences are available upon request.

Statistics. Statistics were computed using Graphpad Prism 7 and 8. *n* refers to the number of individual mice or individual myocyte preparations. All data are expressed as mean ± s.e.m. Repeated symbols are used as follows: single - $p \leq 0.05$; double - $p \leq 0.01$; triple - $p \leq 0.001$. Anderson-Darling (A2*) test was performed to test for normality. If the data passed the normality test, two-sample *t*-test was used for simple pairwise comparisons, and 1-way ANOVA for the analysis of experiments with more than two groups; if normality testing failed, then the data were analyzed by non-parametric Mann-Whitney test or Kruskal-Wallis Test followed by Dunn's Post-hoc testing, respectively. ANOVA was performed with matching for experiments involving biological replicates based upon separate myocyte preparations. 2-way ANOVA was used for experiments with 2-factor design. All datasets involving multiple comparisons for which *p*-values are provided were significant by ANOVA or Kruskal-Wallis testing, $\alpha = 0.05$. *p*-values for experiments involving multiple comparisons were obtained by Tukey or Dunn's post-hoc testing, albeit *p*-values for not all comparisons are indicated in the figures and tables. Log-rank (Mantel-Cox) test was used to analyze Kaplan-Meier survival curves.

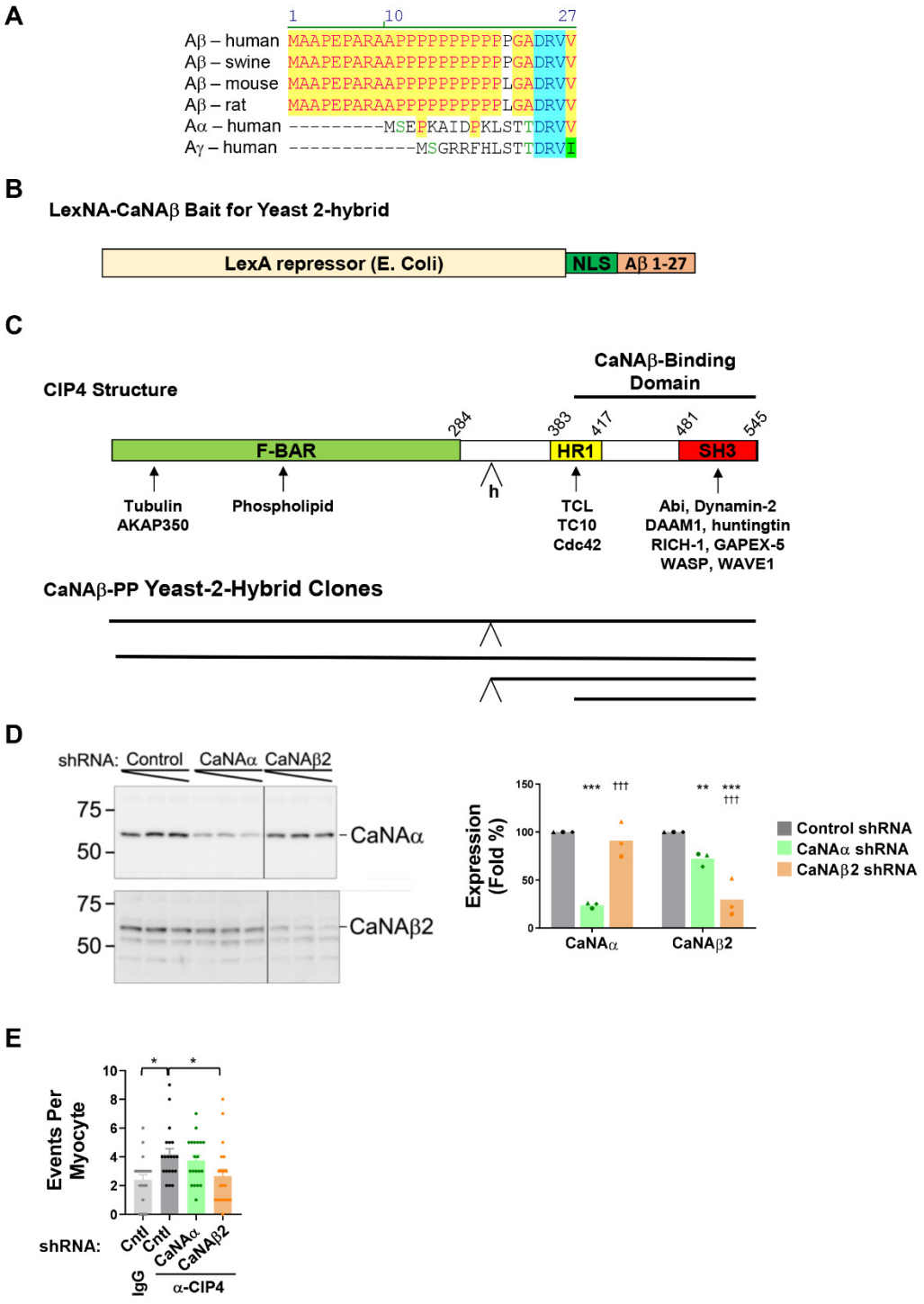

Supplemental Figure I. **Discovery of CIP4 as a CaNAβ scaffold. A.** Alignment of N-terminal sequences for human calcineurin A-subunit isoforms and CaNAβ from select species. **B.** The N-terminal CaNAβ PP peptide fused to a LexA repressor with a nuclear localization site.[41] was used as a bait in a yeast two-hybrid screen. **C.** CIP4 structure and alignment with the four clones isolated by yeast two-hybrid. The arrowhead with an "h" indicates the 56 aa insertion in CIP4a introduced by alternative splicing that constitutes

the CIP4h isoform. CIP4 has a FES/CIP4 homology-Bin/Amphiphysin/Rvs (F-BAR) N-terminal domain, a middle protein kinase C-related kinase homology region 1 (HR1) domain, and a C-terminal Src homology 3 (SH3) domain. Known protein and lipid binding partners are indicated. **D.** Neonatal myocytes were infected with adenovirus expressing CaNAα, CaNAβ2, or control shRNA at a multiplicity of infection (MOI) of 50, 100, 200 and detected with both CaNAα and CaNAβ2 antibodies. The vertical line on the representative blots to the left indicates where non-adjacent lanes of the same gel are shown. Note that only the single band indicated by the CaNAβ2 marker and at the expected molecular weight (59 kDa) was decreased with the CaNAβ2 shRNA. Bars and symbols on graph on right indicate average mean and values for independent experiments using different myocyte preparations, respectively, for fold expression for highest virus MOI. *n* = 3. * vs. control shRNA; † vs. CaNAα shRNA. Data analyzed by two-way ANOVA with matching for each separate experiment and Tukey post-hoc testing for differences in detection with each antibody. **E.** Detection of endogenous calcineurin-CIP4 complexes by proximity ligation assay with mouse α-CIP4 and rabbit α-CaNAβ2 antibodies in adult rat ventricular myocytes infected with shRNA adenovirus. Representative experiment of 2 replicates shown. Data analyzed by Kruskal-Wallis and Dunn's post-hoc testing.

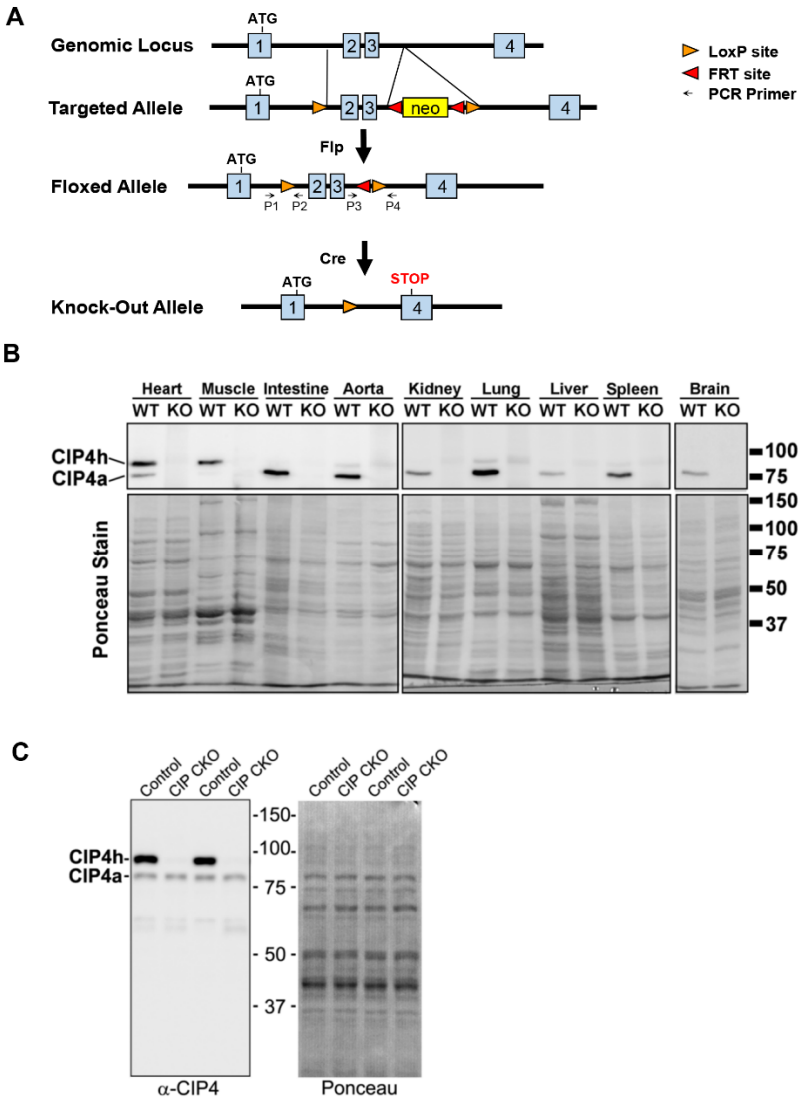

Supplemental Figure II. **Generation of conditional CIP4 knockout mouse. A.** Schematic of CIP4 genetic locus, targeting vector and knockout allele. Exon 1 encodes aa 1-8, Exon 2 – aa 9-47, Exon 3 - 47- 66, and Exon 4 – aa 66-115. LoxP sites and a neomycin-resistance cassette flanked by FRT sites were inserted by homologous recombination, followed by subsequent FRT recombinase-mediated deletion of the neomycin selection cassette. Cre-mediated recombination results in deletion of exons 2 and 3 and a frameshift in exon 4. **B.** Western blot of tissue extracts from WT and *CIP4*$^{fl/fl}$;Tg(CMV-cre) constitutive knockout mice. CIP4 antibody revealed differential expression of CIP4a and CIP4h in different tissues, with results similar to those previously published.[50] The exposure time for the brain blot was longer than for the others due to the lower expression of CIP4 in that tissue. Total protein was detected by Ponceau stain. **C.** Western blot for CIP4 using heart extracts (25 µg total protein) from CIP4 CKO *CIP4*$^{fl/fl}$;Tg(Myh6-cre/Esr1*) and control Tg(Myh6-cre/Esr1*) mice 3 weeks after tamoxifen administration. These results imply that only CIP4h is expressed in the adult myocyte, unlike the neonatal cardiac myocyte in which CIP4a and CIP4h are both expressed.[25] $n > 4$.

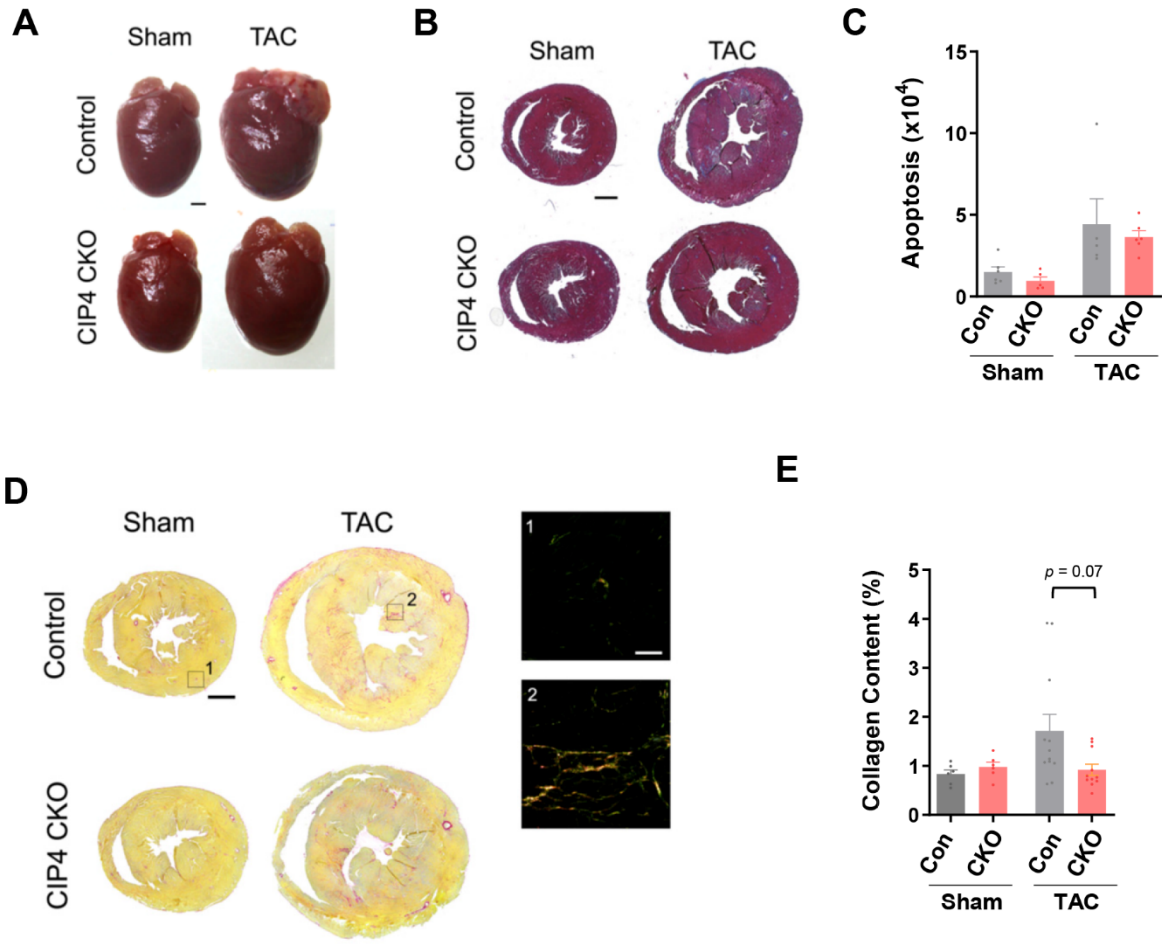

Supplemental Figure III. **Pathologic analysis of CIP4 CKO mice subjected to 16 weeks of pressure overload.** Control mice were MCM. All mice were tamoxifen-treated. **A.** Representative mouse hearts. Scale bar - 1 mm. **B.** Trichrome-stained transverse tissue sections. Scale bar - 1 mm. **C**. TUNEL staining of endpoint hearts for myocardial cell death. *n* = 5-6 mice. **D.** Representative picrosirius red–stained sections imaged with bright field microscopy (left, bar - 1 mm) and circularly polarized light microscopy (examples shown in insets on the right, bar - 100 μm). **E.** Collagen content based upon polarized light microscopy of picrosirius red-stained sections. *n* = 6-12 mice. Data in C and E analyzed by 2-way ANOVA and Tukey post-hoc testing.

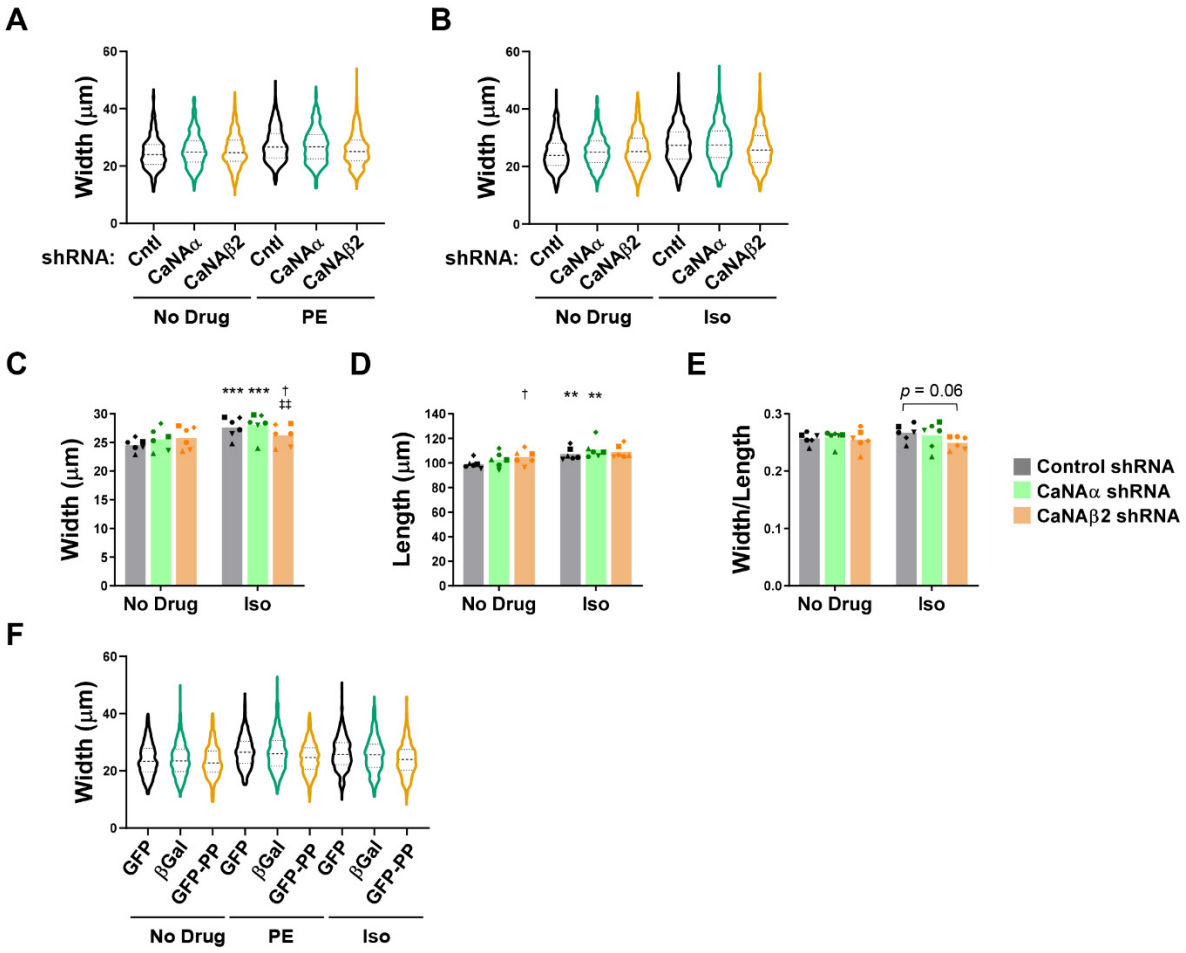

Supplemental Figure IV. **Calcineurin Aβ2-induced myocyte hypertrophy. A.** Distribution for Figure 3B of cell widths over 4 independent experiments. Median and quartiles are indicated by dash lines. *n* of cells in aggregate: control shRNA - 467, CaNAα - shRNA - 453, CaNAβ2-shRNA - 426, Control shRNA + PE - 516, CaNAα - shRNA + PE - 519, CaNAβ2-shRNA + PE – 546. **B-E.** ARVM were infected with adenovirus expressing CaNAα, CaNAβ2, or control shRNA (MOI = 1000) and then stimulated for 24 hours with 10 μM Iso before immunocytochemistry using α-actinin antibodies and Hoechst nuclear stain (not shown). **B.** Distribution of cell widths over 6 independent experiments. *n* (in aggregate): control shRNA - 688, CaNAα - shRNA - 746, CaNAβ2-shRNA - 668, Control shRNA + Iso - 780, CaNAα - shRNA + Iso - 667, CaNAβ2-shRNA + Iso – 768. Median and quartiles are indicated by dash lines. **C-E.** Bars and symbols indicate average mean and means of independent experiments using different myocyte preparations, respectively, for width (C), length (D), and width/length ratio (E) are shown. *n* = 6 independent experiments. **p*-value vs. no drug control for the same shRNA. † vs. control shRNA under the same treatment condition; ‡ vs. CaNAα shRNA under the same treatment condition. Data were analyzed by 2-way ANOVA for matched data with Tukey post-hoc testing. **F.** Distribution for Figure 3F of cell widths over 7 independent experiments, Median and quartiles are indicated by dash lines. *n*: GFP - 438, β-gal - 556 (green dashed curve), PP - GFP - 424, GFP + PE - 439, β-gal + PE - 595, PP-GFP + PE – 418, GFP + Iso – 410, β-gal + Iso – 484, PP-GFP + Iso - 422.

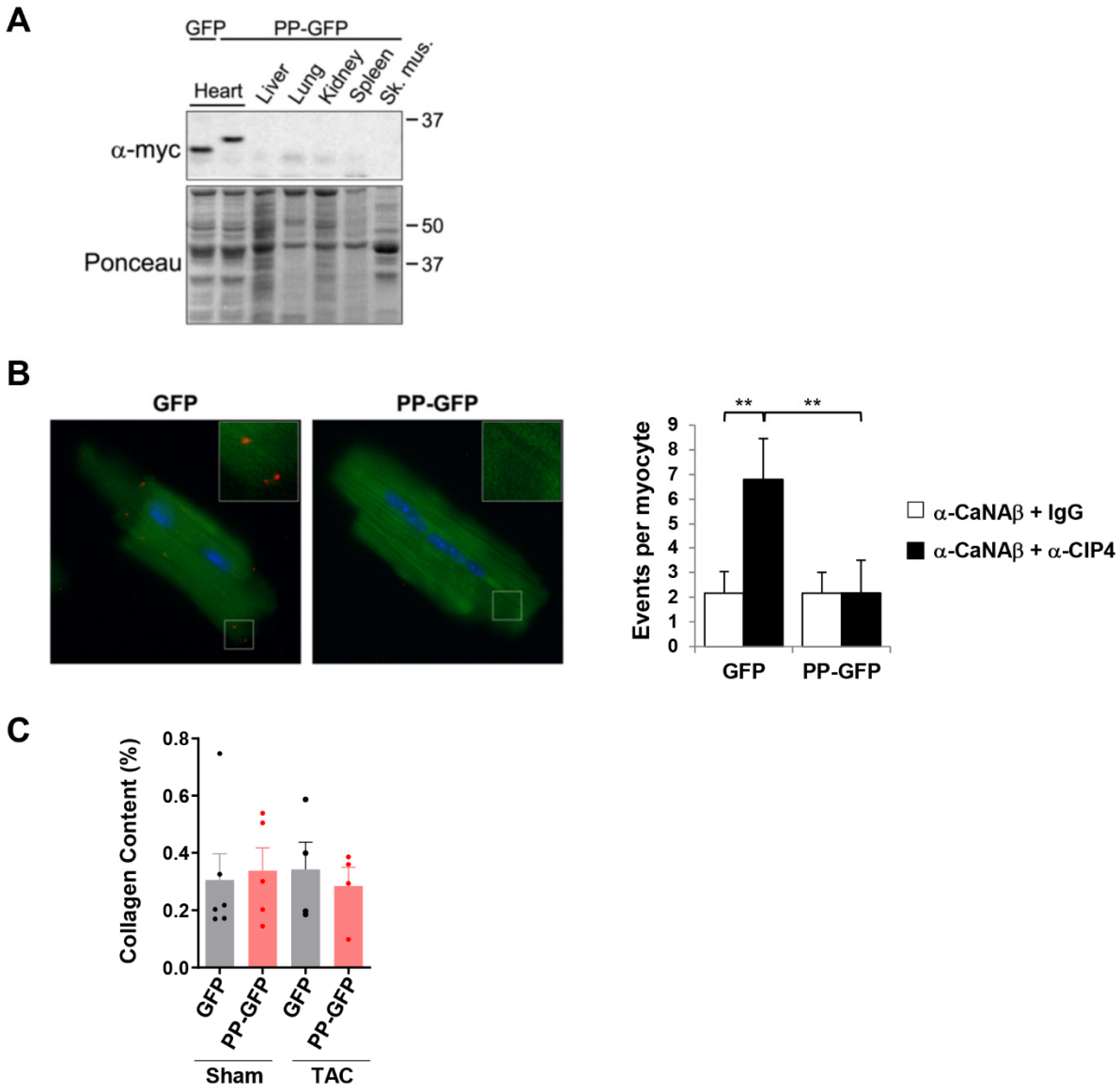

Supplemental Figure V. **Expression *in vivo* by AAV9.PP-GFP. A.** Detection of PP-GFP and GFP by myc tag antibody western blot of tissue extracts. *n* = 3. **B.** Detection by proximity ligation assay with mouse anti-CIP4 and rabbit anti-CaNAβ2 antibodies of endogenous CaNAβ-CIP4 complexes (large red spots) in cardiac myocytes isolated from AAV-injected mice. *n* = 3 mice per AAV. Data by 2-way ANOVA and Tukey post-hoc testing. **C.** Collagen content based upon polarized light microscopy of picrosirius red-stained sections. *n* = 4-6 mice. ANOVA was not significant.

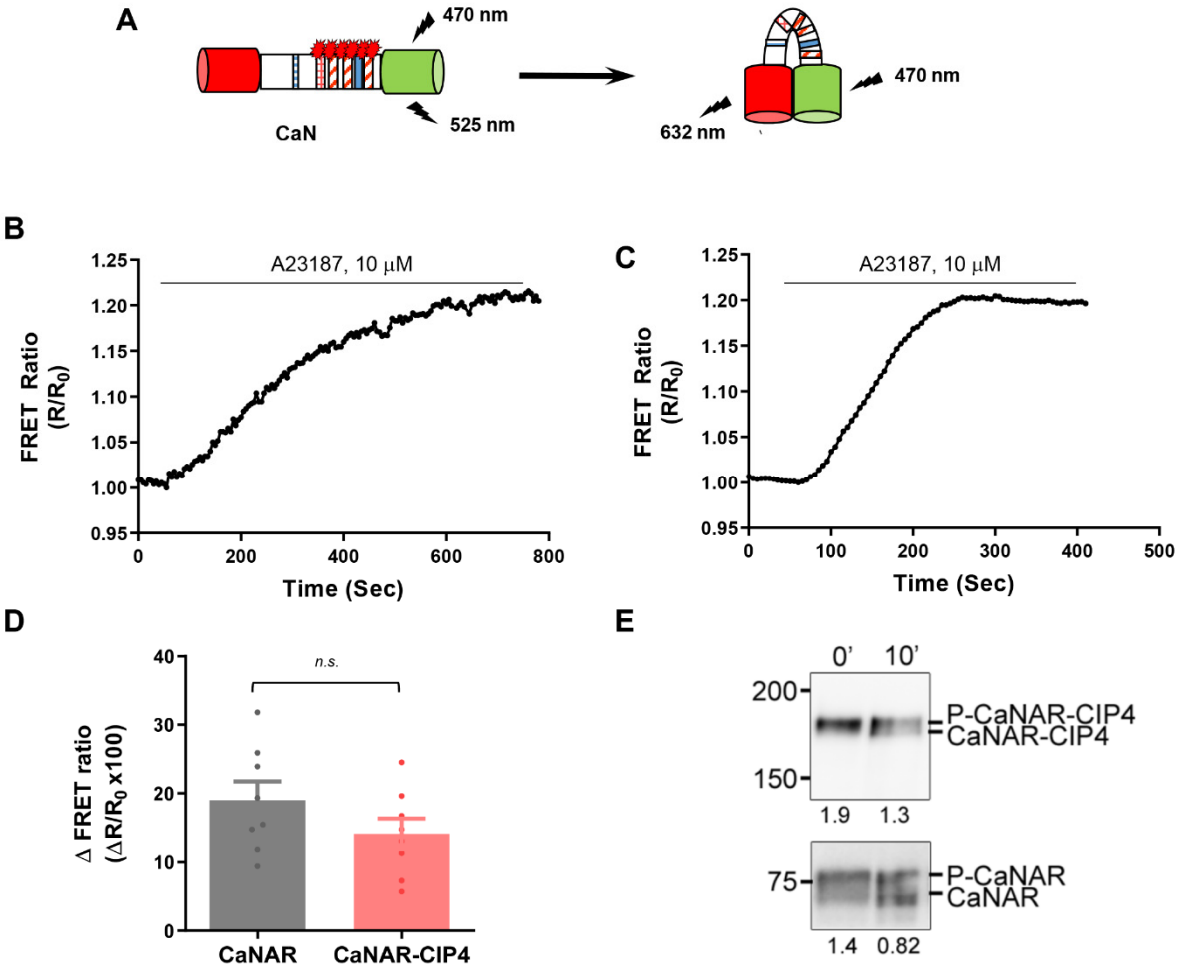

Supplemental Figure VI. **Validation of a new calcineurin activity reporter. A.** Dephosphorylation of the sensor increases EGFP-mCherry FRET activity. **B,C.** HeLa cells were infected with CaNAR (B) and CaNAR-CIP4 (C) adenovirus (MOI = 20) and 48 hours later stimulated with Ca^{2+} ionophore (A23187, 10 μmol/L). Representative tracings and change in peak FRET ratio (R/R_0) are shown. **D.** The peak amplitudes in B & C were similar for the two sensors, showing that both sensors were functional in cells. *n* = 8 tracings from 2 independent experiments. **E.** NFATc1 dephosphorylation confers increased mobility in SDS-PAGE allowing additional validation of the sensors by western blot. COS-7 cells were transfected with expression plasmids for CaNAR and CaNAR-CIP4 and were stimulated for 10 minutes with 2 μmol/L ionomycin and 10 mmol/L $CaCl_2$ before lysis in Laemmlli sample buffer and SDS-PAGE. The CaNAR (bottom) and CaNAR-CIP4 (top) sensors were detected by immunoblot with α-GFP and α-myc tag antibodies, respectively. The ratio of the intensity of the top band to lower band is given below the individual lanes. *n* = 2.

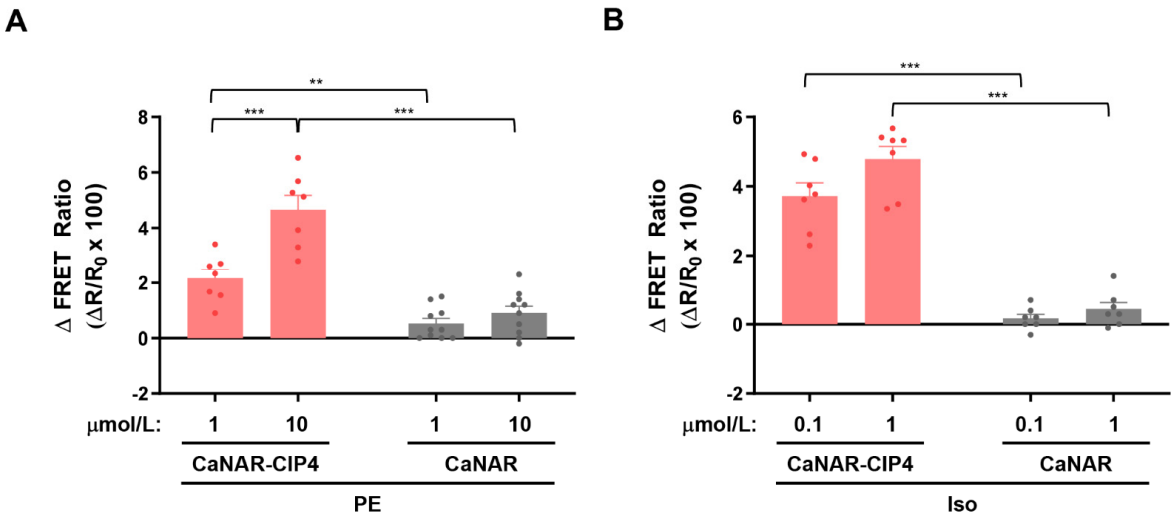

Supplemental Figure VII. **Response of CaNAR and CaNAR-CIP4 to adrenergic agonists.** Myocytes were infected with adenovirus expressing CaNAR or CaNAR-CIP4 FRET sensors and stimulated with phenylephrine (PE, panel A) or isoproterenol (Iso, panel B). Change in FRET ratio for individual tracings and mean ± s.e.m. are indicated. Data were analyzed by two-way ANOVA and Tukey Post-hoc testing.

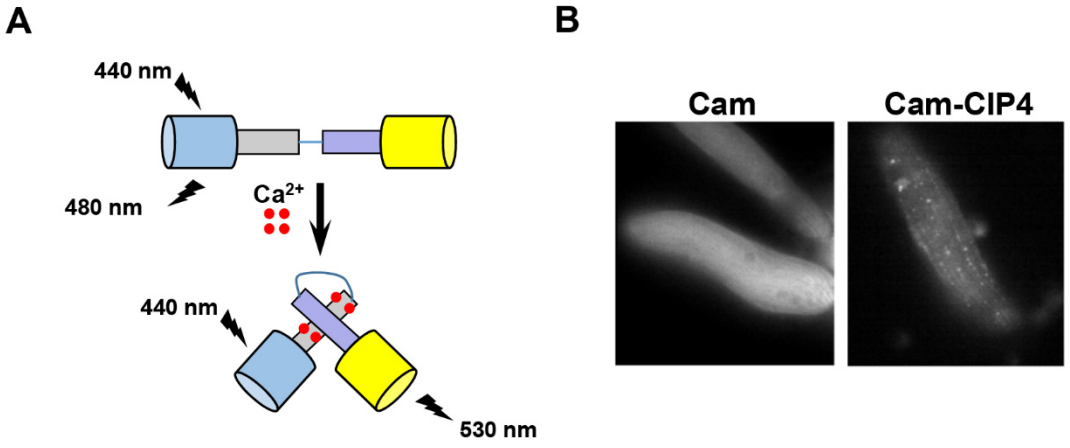

Supplemental Figure VIII. **Cameleon sensors. A.** Ca^{2+}-binding increases ECFP-cp-Venus FRET activity. **B.** Widefield images are shown of Cam and Cam-CIP4 sensors expressed in adult myocytes.

Supplemental Table I: Yeast 2-hybrid screen for CaNAβ polyproline domain interactors.

Gene Name	Protein Names	Consensus PP binding domain	NCBI Acc Number	5' bp for each clone	Alt. Splice Form	Bar Family Members	RPKM in Heart
SORBS2	Sorbs2 (sorbin and SH3 domain containing 2); ArgBP2 (Arg/Abl binding-protein 2)	SH3	NM_001145672	991	variant 5		46.6
			NM_001145671	1204	variant 4		
			NM_003603	1781	variant 1		
				1794			
				1950			
				2002			
PFN1	Profilin -1	profilin	NM_005022	558			36.6
				564			
				564			
				585			
				585			
				591			
TRIP10	CIP4 (Cdc42-interacting protein 4); TRIP10 (thyroid hormone receptor interactor 10)	SH3	NM_001288962	59	variant 1 (h)	F-Bar	18.9
				1120	variant 1 (h)		
				1449	variant 1 (h)		
			NM_004240	104	variant 2 (a)		
PFN2	Profilin-2	profilin	NM_053024	75			16.5
				75			
SPG21	maspardin; SPG21 (spastic paraplegia 21); ACP33	?	NM_016630	292			12.5
				295			
SNX18	SNX18 (sorting nexin 18	SH3	NM_001102575	1		PX-Bar	2.0
				1			
PRPF40A	PRPF401 A (pre-mRNA processing factor 40 homolog A); FBP11 (formin-binding protein 11); HYPA; FLAF1; NY-REN-6	WW	NM_017892	238			4.0
				238			
FNBP1L	FNBP1L (formin binding protein 1 like); TOCA-1 (transducer of Cdc42-dependent actin assembly)	SH3	NM_001024948	797		F-Bar	4.4
MTSS1L	ABBA (actin-bundling protein with BAIAP2 homology)	?	NM_138383	2244		I-Bar	4.9
SDCBP	syndecan binding protein; syntenin; MDA-9	?	NM_005625	394			23.1

Individual pACT2 clones isolated from human heart cDNA library by association with LexNA-CaNAβ PP fusion protein. 5' base pair (bp) for the cDNA in each clone is indicated. Clones with same 5' bp may represent duplicate isolations of same primary clone. 28/31 pACT2 clones that were sequenced contained open reading frames in frame with the LexNA fusion protein. Relative abundance of the respective mRNA in the human heart is indicated as reads per kilobase million (RPKM, NCBI Bioproject PRJEB4337; Fagerberg L *et al.*, *Mol Cell Proteomics*, 2013 Dec 5;13(2):397-406).

Supplemental Table II: 2-week Transverse Aortic Constriction – CIP4 CKO Mouse

		MCM - Sham	*CIP4*$^{f/f}$ - Sham	CKO - Sham	MCM - TAC	*CIP4*$^{f/f}$ - TAC	CKO-TAC
n		19	21	25	27	24	44
Echocardiography							
RC/LC ratio					7.6 ± 0.3	8.2 ± 0.3	7.9 ± 0.2
LVPW;d	mm	0.75 ± 0.02	0.75 ± 0.02	0.73 ± 0.02	1.00 ± 0.03 †††	1.02 ± 0.02 †††	0.91 ± 0.02 ††† * ##
LVPW;s	mm	1.07 ± 0.04	1.04 ± 0.03	1.00 ± 0.03	1.24 ± 0.03 ††	1.23 ± 0.03 ††	1.19 ± 0.02 †††
LVAW;d	mm	0.81 ± 0.02	0.75 ± 0.03	0.77 ± 0.01	1.01 ± 0.02 †††	1.04 ± 0.03 †††	0.97 ± 0.02 †††
LVAW;s	mm	1.19 ± 0.04	1.10 ± 0.03	1.11 ± 0.02	1.39 ± 0.04 ††	1.44 ± 0.04 †††	1.34 ± 0.03 †††
LVID;d	mm	4.06 ± 0.08	4.15 ± 0.07	4.12 ± 0.07	4.00 ± 0.07	4.25 ± 0.11	4.02 ± 0.05
LVID;s	mm	2.84 ± 0.10	2.95 ± 0.09	2.95 ± 0.08	2.98 ± 0.11	3.23 ± 0.15	2.95 ± 0.07
LV Vol;d	µL	74 ± 3	77 ± 3	76 ± 3	71 ± 3	83 ± 5	71 ± 2
LV Vol;s	µL	32 ± 3	35 ± 2	35 ± 2	36 ± 3	45 ± 5	35 ± 2
EF	%	58 ± 2	56 ± 2	55 ± 2	51 ± 3	49 ± 3	52 ± 2
FS	%	30 ± 1	29 ± 1	29 ± 1	26 ± 2	25 ± 2	27 ± 1
LV Mass	mg	94 ± 4	93 ± 3	90 ± 2	130 ± 5 †††	148 ± 6 †††	119 ± 3 ††† ###
LV Mass/BW	mg/g	3.9 ± 0.1	4.1 ± 0.1	3.9 ± 0.1	5.7 ± 0.2 †††	6.2 ± 0.1 †††	5.1 ± 0.1 ††† *** ###
HR	BPM	498 ± 3	496 ± 3	494 ± 3	494 ± 3	499 ± 3	497 ± 3
Gravimetrics							
Ventricular Weight	mg	105 ± 4	102 ± 3	103 ± 3	136 ± 5 †††	154 ± 6 †††	131 ± 3 ††† ###
VW/BW	mg/g	4.5 ± 0.1	4.5 ± 0.1	4.5 ± 0.1	6.1 ± 0.1 †††	6.6 ± 0.1 †††	5.6 ± 0.1 ††† ** ###
Atrial Weight	mg	6.2 ± 0.3	5.6 ± 0.2	5.9 ± 0.2	8.8 ± 0.6 ††	9.1 ± 0.7 †††	7.3 ± 0.3 #
AW/BW	mg/g	0.26 ± 0.01	0.25 ± 0.01	0.25 ± 0.01	0.39 ± 0.02 †††	0.38 ± 0.02 †††	0.31 ± 0.01 † *** ##
Lung Weight	mg	131 ± 3	128 ± 2	132 ± 2	153 ± 9	148 ± 10	134 ± 3
LW/BW	mg/g	5.6 ± 0.1	5.7 ± 0.2	5.8 ± 0.1	6.8 ± 0.3 ††	6.4 ± 0.3	5.8 ± 0.1 **
Body Weight	g	23.5 ± 0.8	22.6 ± 0.7	23.1 ± 0.6	22.3 ± 0.6	23.3 ± 0.8	23.1 ± 0.4
Tibial Length	mm	17.4 ± 0.1	17.3 ± 0.1	17.5 ± 0.1	17.1 ± 0.1	17.1 ± 0.1	17.3 ± 0.1

MCM, Tg(Myh6-cre/Esr1*) mice; CKO - *CIP4*$^{f/f}$;Tg(Myh6-cre/Esr1*) mice; RC/LC ratio – ratio of carotid artery blood flow velocities by Doppler; LVPW, Left ventricular posterior wall thickness; LVAW, left ventricular anterior wall thickness; LVID, Left ventricular internal diameter; d, diastole; s, systole; Vol, Volume; EF, ejection fraction; FS, fractional shortening; VW, ventricular weight; BW; body weight; TL; tibial length; AW, atrial weight; LW, lung weight. All data are mean ± s.e.m. † *p* vs. Sham for same genotype mice; * *p* vs. MCM - TAC; $^{\#}$ *p* vs. *CIP4*$^{f/f}$ - TAC. All data were analyzed by 2-way ANOVA for each parameter, followed by Tukey post-hoc testing.

Supplemental Table III: Gene Expression for 2-week Transverse Aortic Constriction – CIP4 CKO Mouse.

		Control - Sham	CIP4 CKO - Sham		Control - TAC		CIP4 CKO -TAC		
Stress Markers									
‖Nppa	Atrial Natriuretic Peptide	1.00 ± 0.26	0.27 ± 0.06		8.34 ± 1.78	†††	3.49 ± 1.06	†††	***
§Nppb	Brain Natriuretic Peptide	1.00 ± 0.33	0.38 ± 0.07		3.23 ± 0.86	††	1.83 ± 0.24		*
Sarcomeric Proteins									
‖Acta1	Skeletal Muscle α-Actin	1.00 ± 0.19	2.04 ± 0.47		30.19 ± 6.93	†††	20.36 ± 4.38	†††	
‖Actc1	Cardiac Muscle α-Actin	1.00 ± 0.05	1.01 ± 0.04		1.14 ± 0.05	†††	1.15 ± 0.05	†††	
Myh6	Cardiac Muscle α-Myosin Heavy Chain	1.00 ± 0.09	0.90 ± 0.03		0.74 ± 0.09	†††	0.72 ± 0.03	†	
‖§Myh7	Cardiac Muscle β-Myosin Heavy Chain	1.00 ± 0.32	0.42 ± 0.06		8.53 ± 1.43	†††	5.91 ± 1.54	†	
Tnnt2	Cardiac Muscle Troponin T	1.00 ± 0.04	1.20 ± 0.03	***	0.81 ± 0.05	†††	0.94 ± 0.05	†††	***
Calcium Handling									
‖§Atp2a2	Sarco/Endoplasmic Reticulum Ca^{2+}-ATPase 2	1.00 ± 0.03	1.00 ± 0.01		0.72 ± 0.04	†††	0.82 ± 0.01	†††	***
Cacna1c	L-Type Calcium Channel Subunit α1c	1.00 ± 0.07	1.10 ± 0.07		1.15 ± 0.11		1.07 ± 0.03		
‖Pln	Phospholamban	1.00 ± 0.03	1.06 ± 0.03		0.78 ± 0.05	†††	0.88 ± 0.03	†††	***
Trpc3	Transient Receptor Potential Cation Channel C 3	1.00 ± 0.03	0.99 ± 0.10		1.18 ± 0.08		1.37 ± 0.08		
§Trpc6	Transient Receptor Potential Cation Channel C 6	1.00 ± 0.05	1.02 ± 0.04		0.84 ± 0.08		0.90 ± 0.03		
Fibrosis/Extracellular Matrix									
Col1a1	Collagen Type I α1	1.00 ± 0.12	1.08 ± 0.23		4.12 ± 1.07		2.64 ± 0.34		
Col1a2	Collagen Type I α2	1.00 ± 0.07	1.08 ± 0.18		3.38 ± 0.87		2.20 ± 0.27		
Col3a1	Collagen Type III α1	1.00 ± 0.11	1.10 ± 0.28		4.14 ± 1.04		2.74 ± 0.42		
Col5a1	Collagen Type V α1	1.00 ± 0.03	0.85 ± 0.08		1.97 ± 0.30		1.52 ± 0.13		
Col6a1	Collagen Type VI α1	1.00 ± 0.03	1.02 ± 0.11		2.15 ± 0.24		1.79 ± 0.11		
Col8a1	Collagen Type VIII α1	1.00 ± 0.05	1.09 ± 0.12		5.93 ± 1.12		3.64 ± 0.59		
Eln	Elastin	1.00 ± 0.37	0.95 ± 0.11		4.16 ± 1.32		2.33 ± 0.33		
Fbn1	Fibrillin-1	1.00 ± 0.11	0.89 ± 0.21		3.25 ± 0.50		2.10 ± 0.28		
Fn1	Fibronectin 1	1.00 ± 0.05	1.05 ± 0.06		4.20 ± 1.52		2.28 ± 0.23		
Ltbp2	Latent Transforming Growth Factor β Binding Protein 2	1.00 ± 0.22	0.73 ± 0.16		20.17 ± 7.89		7.07 ± 1.91		
Mfap5	Microfibrillar Associated Protein 5	1.00 ± 0.03	0.90 ± 0.12		3.68 ± 0.74		2.46 ± 0.30		
Mmp2	Matrix Metallopeptidase 2	1.00 ± 0.04	1.00 ± 0.05		2.40 ± 0.26		1.73 ± 0.11		
‖Pcolce	Procollagen C-Endopeptidase Enhancer	1.00 ± 0.04	1.07 ± 0.11		1.92 ± 0.23		1.62 ± 0.13		
Postn	Periostin	1.00 ± 0.07	0.91 ± 0.09		9.29 ± 2.61		4.85 ± 1.36		
Tnc	Tenascin C	1.00 ± 0.15	0.76 ± 0.11		7.67 ± 2.32		3.71 ± 0.93		
Tgfb1	Transforming Growth Factor β1	1.00 ± 0.03	0.97 ± 0.04		1.43 ± 0.11		1.37 ± 0.06		
Tgfb2	Transforming Growth Factor β2	1.00 ± 0.07	0.84 ± 0.14		3.04 ± 0.65		1.84 ± 0.18		
Cell Survival/Death Pathways									
Casp8	Caspase 8	1.00 ± 0.04	0.86 ± 0.10		1.43 ± 0.15		1.39 ± 0.11		
Casp9	Caspase 9	1.00 ± 0.07	1.03 ± 0.06		1.14 ± 0.08		1.07 ± 0.03		
Bad	BCL2-Associated Agonist Of Cell Death	1.00 ± 0.05	1.05 ± 0.04		1.20 ± 0.07		1.19 ± 0.03		
Bax	BCL2-Associated X Protein	1.00 ± 0.08	0.88 ± 0.03		1.35 ± 0.11		1.21 ± 0.07		
§Bcl-2	B Cell Leukemia/Lymphoma 2	1.00 ± 0.10	0.75 ± 0.06		1.96 ± 0.24		1.37 ± 0.09		

Signal Transduction					
Adra1a	α1-Adrenergic Receptor	1.00 ± 0.05	1.40 ± 0.15	0.66 ± 0.11	0.94 ± 0.09
Adrb1	β1-Adrenergic Receptor	1.00 ± 0.07	0.82 ± 0.11	0.66 ± 0.02	0.86 ± 0.04
Adrb2	β2-Adrenergic Receptor	1.00 ± 0.05	0.96 ± 0.04	1.18 ± 0.07	1.22 ± 0.05
Bin1	Amphiphysin II	1.00 ± 0.03	0.94 ± 0.03	1.40 ± 0.10	1.42 ± 0.04
Cabin1	Calcineurin Binding Protein 1	1.00 ± 0.04	1.06 ± 0.08	1.09 ± 0.04	1.12 ± 0.04
Camk2d	Calcium/Calmodulin-Dependent Protein Kinase II δ	1.00 ± 0.03	0.99 ± 0.06	1.03 ± 0.03	1.05 ± 0.03
‖Dusp6	Dual Specificity Protein Phosphatase 6	1.00 ± 0.06	0.81 ± 0.05	1.26 ± 0.12	1.04 ± 0.08
Fhl1	Four And A Half LIM Domains Protein 1	1.00 ± 0.06	1.17 ± 0.09	2.63 ± 0.44	1.81 ± 0.17
Mapk3	Erk1	1.00 ± 0.03	1.09 ± 0.03	1.19 ± 0.07	1.27 ± 0.04
Mapk1	Erk2	1.00 ± 0.02	1.11 ± 0.02	0.98 ± 0.03	1.09 ± 0.04
Mapk8	Jnk1	1.00 ± 0.02	1.05 ± 0.06	1.07 ± 0.03	1.14 ± 0.06
Mapk9	Jnk2	1.00 ± 0.04	1.10 ± 0.05	0.99 ± 0.05	1.06 ± 0.03
Mapk10	Jnk3	1.00 ± 0.04	1.25 ± 0.09	0.98 ± 0.08	1.13 ± 0.04
Mapk14	p38α	1.00 ± 0.07	0.98 ± 0.07	0.77 ± 0.04	0.90 ± 0.06
Mapk11	p38β	1.00 ± 0.06	0.91 ± 0.05	1.06 ± 0.11	1.09 ± 0.06
§‖Myoz2	Calsarcin-1	1.00 ± 0.04	0.97 ± 0.03	1.15 ± 0.06	1.13 ± 0.04
§‖Ppp3cb	Calcineurin Aβ Catalytic Subunit	1.00 ± 0.02	0.96 ± 0.01	0.91 ± 0.02	0.92 ± 0.02
§Rcan1	Regulator Of Calcineurin 1	1.00 ± 0.20	0.78 ± 0.07	3.45 ± 1.27	1.50 ± 0.24
Trip10	Cip4	1.00 ± 0.08	1.78 ± 0.31	0.86 ± 0.09	1.52 ± 0.16
Vegfa	Vascular Endothelial Growth Factor A	1.00 ± 0.07	0.83 ± 0.04	1.05 ± 0.12	0.97 ± 0.04
Transcription Factors					
§Hand2	Heart And Neural Crest Derivatives Expressed 2	1.00 ± 0.08	0.93 ± 0.04	0.77 ± 0.08	0.83 ± 0.07
Hif1a	Hypoxia Inducible Factor 1α	1.00 ± 0.02	1.18 ± 0.09	1.32 ± 0.09	1.45 ± 0.13
‖Mef2a	Myocyte Enhancer Factor 2a	1.00 ± 0.08	1.04 ± 0.04	1.07 ± 0.06	1.10 ± 0.04
Mef2c	Myocyte Enhancer Factor 2c	1.00 ± 0.03	1.05 ± 0.09	1.06 ± 0.05	1.10 ± 0.04
Mef2d	Myocyte Enhancer Factor 2d	1.00 ± 0.03	1.12 ± 0.05	2.26 ± 0.32	1.90 ± 0.22
Nfatc1	Nuclear Factor Of Activated T Cells Type 1	1.00 ± 0.03	1.15 ± 0.05	1.08 ± 0.04	1.22 ± 0.05
Nfatc2	Nuclear Factor Of Activated T Cells Type 2	1.00 ± 0.12	1.07 ± 0.04	0.88 ± 0.07	0.91 ± 0.05
Nfatc3	Nuclear Factor Of Activated T Cells Type 3	1.00 ± 0.05	1.14 ± 0.05	1.07 ± 0.05	1.27 ± 0.06
Nfatc4	Nuclear Factor Of Activated T Cells Type 4	1.00 ± 0.08	1.07 ± 0.08	1.46 ± 0.11	1.30 ± 0.08
‖Nkx2-5	Nkx2.5 Homeobox	1.00 ± 0.00	0.97 ± 0.03	0.84 ± 0.03	0.93 ± 0.02
Miscellaneous					
Slc2a1	Glucose Transporter 1	1.00 ± 0.09	1.10 ± 0.04	1.04 ± 0.09	1.02 ± 0.04
‖Slc2a4	Glucose Transporter 4	1.00 ± 0.06	1.05 ± 0.06	0.74 ± 0.06	0.77 ± 0.04

Total mouse left ventricular RNA was assayed by NanoString technology for the indicated mRNAs and normalized to *Hprt* mRNA levels. Genes marked with "§" and "‖" are known NFATc and MEF2 target genes, respectively. Control mice were tamoxifen-treated Tg(Myh6-cre/Esr1*) mice. All data (mean ± s.e.m.) are fold-expression compared to the Control Sham cohort. *n* = 4 for Sham cohorts; *n* = 6 for TAC cohorts. † *p* vs. sham-operated for same genotype mice; * *p* vs. control mice for same treatment. 2-way ANOVA with matching for each mouse was performed with Tukey post-hoc testing for differences within rows using data before normalization to the Control Sham cohort.

Supplemental Table IV: 16-week Transverse Aortic Constriction – CIP4 CKO Mouse

		Control - Sham	CKO - Sham	Control - TAC	CKO - TAC
Echocardiography					
n		11	16	25	33
LVPW;d	mm	0.75 ± 0.02	0.83 ± 0.03	1.07 ± 0.03 †††	1.08 ± 0.02 †††
LVPW;s	mm	1.06 ± 0.04	1.08 ± 0.06	1.17 ± 0.04	1.20 ± 0.02
LVAW;d	mm	0.95 ± 0.04	0.95 ± 0.04	1.17 ± 0.04 ††	1.19 ± 0.03 †††
LVAW;s	mm	1.34 ± 0.04	1.35 ± 0.06	1.40 ± 0.05	1.45 ± 0.04
LVID;d	mm	3.91 ± 0.07	4.03 ± 0.11	4.94 ± 0.15 †††	4.85 ± 0.13 †††
LVID;s	mm	2.66 ± 0.10	2.87 ± 0.15	4.32 ± 0.18 †††	4.15 ± 0.16 †††
LV Vol;d	µL	67 ± 3	72 ± 4	119 ± 9 ††	114 ± 8 ††
LV Vol;s	µL	27 ± 2	33 ± 3	89 ± 10 †††	82 ± 8 †††
EF	%	61 ± 2	56 ± 3	28 ± 2 †††	32 ± 2 †††
FS	%	32 ± 2	29 ± 2	13 ± 1 †††	15 ± 1 †††
LV Mass	mg	98 ± 4	110 ± 4	211 ± 9 †††	210 ± 9 †††
LV Mass/BW	mg/g	3.6 ± 0.1	4.2 ± 0.1	9.4 ± 0.6 †††	8.1 ± 0.4 †††
HR	BPM	498 ± 4	500 ± 3	495 ± 6	502 ± 2
RC/LC ratio (2 weeks post-TAC)				8.46 ± 0.26	8.42 ± 0.25
Gravimetrics					
n		11	16	24	33
Ventricular Weight	mg	103 ± 4	113 ± 4	200 ± 8 †††	203 ± 8 †††
VW/BW	mg/g	3.87 ± 0.04	4.33 ± 0.08	8.83 ± 0.47 †††	7.91 ± 0.38 †††
VW/TL	mg/mm	5.8 ± 0.2	6.5 ± 0.2	11.5 ± 0.5 †††	11.7 ± 0.5 †††
Atrial Weight	mg	6.0 ± 0.2	6.1 ± 0.3	33.1 ± 4.5 †††	17.6 ± 3.0 **
AW/BW	mg/g	0.23 ± 0.01	0.23 ± 0.01	1.55 ± 0.24 †††	0.72 ± 0.14 **
AW/TL	mg/mm	0.34 ± 0.01	0.35 ± 0.02	1.90 ± 0.26 †††	1.02 ± 0.17 **
Lung Weight	mg	136 ± 4	138 ± 4	295 ± 26 †††	209 ± 19 **
LW/BW	mg/g	5.2 ± 0.2	5.3 ± 0.2	13.5 ± 1.5 †††	8.5 ± 1.0 **
LW/TL	mg/mm	7.8 ± 0.2	8.0 ± 0.2	16.9 ± 1.5 †††	12.1 ± 1.1 *
Body Weight	g	26.6 ± 1.2	26.1 ± 0.9	23.4 ± 0.9	26.1 ± 0.7
Tibial Length	mm	17.56 ± 0.10	17.31 ± 0.11	17.44 ± 0.06	17.34 ± 0.06

Control mice were tamoxifen-treated Tg(Myh6-cre/Esr1*) mice. Abbreviations: RC/LC ratio – ratio of carotid artery blood flow velocities for entire cohorts by Doppler 2 weeks post-TAC; LVPW, left ventricular posterior wall thickness; LVAW, left ventricular anterior wall thickness; LVID, Left ventricular internal diameter; d, diastole; s, systole; Vol, Volume; EF, ejection fraction; FS, fractional shortening; VW, biventricular weight; BW; body weight; TL; tibial length; AW, atrial weight; LW, lung weight. All data are mean ± s.e.m. and with the exception of RC/LC ratio were obtained 16 weeks post-operatively. † *p* vs. Sham for same genotype mice; * *p* vs Control - TAC. All data were analyzed by 2-way ANOVA for each parameter, followed by Tukey post-hoc testing.

Supplemental Table V: 2-week Transverse Aortic Constriction – AAV9.PP-GFP

		GFP - Sham	PP-GFP - Sham	GFP - TAC		PP-GFP - TAC		
n		20	17	24		22		
Echocardiography								
RC/LC ratio				8.3 ± 0.3		8.3 ± 0.4		
LVPW;d	mm	0.74 ± 0.02	0.71 ± 0.01	0.93 ± 0.01	†††	0.94 ± 0.02	†††	
LVPW;s	mm	1.06 ± 0.03	0.96 ± 0.03	1.05 ± 0.02		1.18 ± 0.04	†††	**
LVAW;d	mm	0.79 ± 0.02	0.73 ± 0.02	1.03 ± 0.02	†††	1.00 ± 0.02	†††	
LVAW;s	mm	1.16 ± 0.03	1.09 ± 0.04	1.42 ± 0.04	†††	1.45 ± 0.04	†††	
LVID;d	mm	3.99 ± 0.07	4.19 ± 0.06	4.25 ± 0.09		4.03 ± 0.05		
LVID;s	mm	2.82 ± 0.10	3.05 ± 0.10	3.32 ± 0.13	††	2.90 ± 0.07		*
LV Vol;d	µL	70 ± 3	79 ± 3	82 ± 4	†	71 ± 2		
LV Vol;s	µL	31 ± 3	37 ± 3	47 ± 4	††	33 ± 2		**
EF	%	57 ± 3	53 ± 2	45 ± 2	††	54 ± 2		*
FS	%	30 ± 2	27 ± 2	22 ± 1	††	28 ± 1		*
LV Mass	mg	88 ± 3	88 ± 2	138 ± 6	†††	125 ± 3	†††	
LV Mass/BW	mg/g	4.02 ± 0.06	4.23 ± 0.12	6.39 ± 0.13	†††	5.77 ± 0.15	†††	**
HR	BPM	498 ± 3	497 ± 2	496 ± 3		492 ± 3		
Gravimetrics								
Ventricular Weight	mg	102 ± 4	100 ± 3	143 ± 6	†††	131 ± 3	†††	
VW/BW	mg/g	4.7 ± 0.1	4.9 ± 0.1	6.7 ± 0.2	†††	6.2 ± 0.1	†††	*
Atrial Weight	mg	6.5 ± 0.3	6.2 ± 0.4	8.1 ± 0.6		7.1 ± 0.3		
AW/BW	mg/g	0.30 ± 0.01	0.30 ± 0.01	0.38 ± 0.02	††	0.34 ± 0.01		
Lung Weight	mg	126 ± 3	124 ± 2	129 ± 5		125 ± 3		
LW/BW	mg/g	5.9 ± 0.1	6.0 ± 0.1	6.1 ± 0.2		5.9 ± 0.1		
Body Weight	g	21.6 ± 0.8	20.8 ± 0.7	21.2 ± 0.7		21.2 ± 0.7		
Tibial Length	mm	16.7 ± 0.1	16.4 ± 0.1	16.3 ± 0.1	†	16.4 ± 0.1		

RC/LC ratio – ratio of carotid artery blood flow velocities by Doppler; LVPW, Left ventricular posterior wall thickness; LVAW, left ventricular anterior wall thickness; LVID, Left ventricular internal diameter; d, diastole; s, systole; Vol, Volume; EF, ejection fraction; FS, fractional shortening; VW, ventricular weight; BW; body weight; TL; tibial length; AW, atrial weight; LW, lung weight. All data are mean ± s.e.m. † *p* vs. Sham with same virus; * *p* vs. GFP-TAC. All data were analyzed by 2-way ANOVA for each parameter, followed by Tukey post-hoc testing.

Supplemental Table VI: Gene Expression for 2-week Transverse Aortic Constriction - AAV9.PP-GFP

		GFP - Sham	PP-GFP - Sham	GFP - TAC	PP-GFP -TAC	
Stress Markers						
‖Nppa	Atrial Natriuretic Peptide	1.00 ± 0.16	0.86 ± 0.09	9.96 ± 3.12 †††	3.99 ± 0.49 †††	***
§Nppb	Brain Natriuretic Peptide	1.00 ± 0.23	1.22 ± 0.36	5.75 ± 0.49 ††	4.88 ± 0.66 †	
Sarcomeric Proteins						
‖Acta1	Skeletal Muscle α-Actin	1.00 ± 0.36	0.96 ± 0.26	10.61 ± 1.99 †††	9.90 ± 2.41 †††	
‖Actc1	Cardiac Muscle α-Actin	1.00 ± 0.11	1.04 ± 0.02	1.12 ± 0.02 †††	1.15 ± 0.03 †††	
Myh6	Cardiac Muscle α-Myosin Heavy Chain	1.00 ± 0.03	0.92 ± 0.03	0.74 ± 0.01 †††	0.84 ± 0.04	
§‖Myh7	Cardiac Muscle β-Myosin Heavy Chain	1.00 ± 0.17	0.88 ± 0.12	9.70 ± 2.74 †	5.16 ± 1.02	
Tnnt2	Cardiac Muscle Troponin T	1.00 ± 0.04	1.01 ± 0.05	0.79 ± 0.01 †††	0.85 ± 0.03 †††	**
Calcium Handling						
§‖Atp2a2	Sarco/Endoplasmic Reticulum Ca2+-ATPase 2	1.00 ± 0.06	0.98 ± 0.02	0.66 ± 0.03 †††	0.76 ± 0.03 †††	***
Cacna1c	L-Type Calcium Channel Subunit α1c	1.00 ± 0.07	0.87 ± 0.05	1.00 ± 0.06	1.04 ± 0.06	
‖Pln	Phospholamban	1.00 ± 0.05	0.96 ± 0.03	0.71 ± 0.02 †††	0.79 ± 0.03 †††	***
Trpc3	Transient Receptor Potential Cation Channel C 3	1.00 ± 0.04	0.83 ± 0.08	1.04 ± 0.05	1.12 ± 0.07	
§Trpc6	Transient Receptor Potential Cation Channel C 6	1.00 ± 0.01	0.99 ± 0.06	0.69 ± 0.06	0.79 ± 0.04	
Fibrosis/Extracellular Matrix						
Col1a1	Collagen Type I α1	1.00 ± 0.20	1.01 ± 0.14	3.47 ± 0.88	2.34 ± 0.25	
Col1a2	Collagen Type I α2	1.00 ± 0.08	0.98 ± 0.13	2.77 ± 0.67	1.86 ± 0.21	
Col3a1	Collagen Type III α1	1.00 ± 0.31	1.07 ± 0.18	3.34 ± 0.68	2.47 ± 0.28	
Col5a1	Collagen Type V α1	1.00 ± 0.12	1.00 ± 0.07	1.83 ± 0.24	1.56 ± 0.10	
Col6a1	Collagen Type VI α1	1.00 ± 0.13	1.04 ± 0.12	1.98 ± 0.32	1.72 ± 0.09	
Col8a1	Collagen Type VIII α1	1.00 ± 0.04	0.96 ± 0.15	4.66 ± 0.74	3.53 ± 0.79	
Eln	Elastin	1.00 ± 0.17	1.17 ± 0.29	5.33 ± 1.48	3.80 ± 0.61	
Fbn1	Fibrillin-1	1.00 ± 0.22	1.08 ± 0.21	3.24 ± 0.30	2.95 ± 0.34	
Fn1	Fibronectin 1	1.00 ± 0.06	1.04 ± 0.09	2.63 ± 0.47	1.93 ± 0.15	
Ltbp2	Latent Transforming Growth Factor β Binding Protein 2	1.00 ± 0.31	1.54 ± 0.40	23.81 ± 9.48	8.60 ± 2.29	
Mfap5	Microfibrillar Associated Protein 5	1.00 ± 0.13	1.04 ± 0.11	2.87 ± 0.39	2.34 ± 0.26	
Mmp2	Matrix Metallopeptidase 2	1.00 ± 0.02	0.98 ± 0.07	1.89 ± 0.38	1.44 ± 0.10	
‖Pcolce	Procollagen C-Endopeptidase Enhancer	1.00 ± 0.14	1.06 ± 0.07	1.81 ± 0.16	1.61 ± 0.14	
Postn	Periostin	1.00 ± 0.08	1.00 ± 0.14	6.68 ± 1.25	4.55 ± 1.47	
Tnc	Tenascin C	1.00 ± 0.18	1.50 ± 0.28	5.03 ± 0.91	4.61 ± 1.95	
Tgfb1	Transforming Growth Factor β1	1.00 ± 0.09	0.94 ± 0.06	1.21 ± 0.07	1.26 ± 0.08	
Tgfb2	Transforming Growth Factor β2	1.00 ± 0.17	1.12 ± 0.02	2.02 ± 0.24	1.77 ± 0.21	
Cell Survival/Death Pathways						
Casp8	Caspase 8	1.00 ± 0.10	1.09 ± 0.18	1.21 ± 0.10	1.35 ± 0.11	
Casp9	Caspase 9	1.00 ± 0.04	0.90 ± 0.07	0.96 ± 0.07	0.95 ± 0.06	
Bad	BCL2-Associated Agonist Of Cell Death	1.00 ± 0.03	0.91 ± 0.03	1.06 ± 0.05	1.07 ± 0.03	
Bax	BCL2-Associated X Protein	1.00 ± 0.04	1.07 ± 0.08	1.12 ± 0.07	1.14 ± 0.06	
§Bcl-2	B Cell Leukemia/Lymphoma 2	1.00 ± 0.11	0.85 ± 0.08	1.50 ± 0.20	1.24 ± 0.06	

Signal Transduction					
Adra1a	α1-Adrenergic Receptor	1.00 ± 0.11	0.91 ± 0.12	0.62 ± 0.03	0.70 ± 0.06
Adrb1	β1-Adrenergic Receptor	1.00 ± 0.09	0.89 ± 0.07	0.81 ± 0.04	0.89 ± 0.04
Adrb2	β2-Adrenergic Receptor	1.00 ± 0.02	1.02 ± 0.05	1.02 ± 0.08	1.04 ± 0.04
Bin1	Amphiphysin II	1.00 ± 0.10	0.89 ± 0.03	1.16 ± 0.06	1.20 ± 0.04
Cabin1	Calcineurin Binding Protein 1	1.00 ± 0.09	0.97 ± 0.06	0.96 ± 0.05	1.01 ± 0.05
Camk2d	Calcium/Calmodulin-Dependent Protein Kinase II δ	1.00 ± 0.06	0.99 ± 0.02	1.01 ± 0.02	1.08 ± 0.04
Dusp6	Dual Specificity Protein Phosphatase 6	1.00 ± 0.07	0.96 ± 0.10	1.06 ± 0.06	1.09 ± 0.05
Fhl1	Four And A Half LIM Domains Protein 1	1.00 ± 0.03	0.98 ± 0.01	1.73 ± 0.17	1.86 ± 0.31
Mapk3	Erk1	1.00 ± 0.07	0.96 ± 0.04	1.03 ± 0.05	1.07 ± 0.05
Mapk1	Erk2	1.00 ± 0.05	0.94 ± 0.03	0.87 ± 0.02	0.95 ± 0.03
Mapk8	Jnk1	1.00 ± 0.04	0.94 ± 0.03	0.93 ± 0.03	1.01 ± 0.04
Mapk9	Jnk2	1.00 ± 0.02	0.92 ± 0.02	0.85 ± 0.02	0.94 ± 0.04
Mapk10	Jnk3	1.00 ± 0.09	0.97 ± 0.05	0.97 ± 0.03	1.01 ± 0.04
Mapk14	p38α	1.00 ± 0.06	0.95 ± 0.01	0.72 ± 0.02	0.80 ± 0.03
Mapk11	p38β	1.00 ± 0.17	1.24 ± 0.10	1.27 ± 0.13	1.16 ± 0.08
§‖Myoz2	Calsarcin-1	1.00 ± 0.06	0.97 ± 0.08	1.04 ± 0.03	1.13 ± 0.05
§‖Ppp3cb	Calcineurin Aβ Catalytic Subunit	1.00 ± 0.06	0.92 ± 0.01	0.83 ± 0.03	0.89 ± 0.03
§Rcan1	Regulator Of Calcineurin 1	1.00 ± 0.09	1.06 ± 0.06	1.58 ± 0.14	1.97 ± 0.31
Trip10	Cip4	1.00 ± 0.05	0.89 ± 0.07	0.71 ± 0.03	0.76 ± 0.05
Vegfa	Vascular Endothelial Growth Factor A	1.00 ± 0.06	0.97 ± 0.11	1.02 ± 0.04	1.03 ± 0.03
Transcription Factors					
§Hand2	Heart And Neural Crest Derivatives Expressed 2	1.00 ± 0.10	1.05 ± 0.04	0.89 ± 0.06	1.02 ± 0.05
Hif1a	Hypoxia Inducible Factor 1α	1.00 ± 0.02	0.85 ± 0.03	0.98 ± 0.07	0.96 ± 0.06
‖Mef2a	Myocyte Enhancer Factor 2a	1.00 ± 0.05	0.99 ± 0.01	1.02 ± 0.05	1.06 ± 0.04
Mef2c	Myocyte Enhancer Factor 2c	1.00 ± 0.06	0.94 ± 0.04	0.93 ± 0.04	0.99 ± 0.06
Mef2d	Myocyte Enhancer Factor 2d	1.00 ± 0.05	0.93 ± 0.03	1.90 ± 0.23	1.88 ± 0.27
Nfatc1	Nuclear Factor Of Activated T Cells Type 1	1.00 ± 0.05	0.96 ± 0.03	0.99 ± 0.06	0.93 ± 0.06
Nfatc2	Nuclear Factor Of Activated T Cells Type 2	1.00 ± 0.01	1.00 ± 0.03	0.85 ± 0.03	0.86 ± 0.03
Nfatc3	Nuclear Factor Of Activated T Cells Type 3	1.00 ± 0.04	0.89 ± 0.04	0.89 ± 0.05	0.95 ± 0.03
Nfatc4	Nuclear Factor Of Activated T Cells Type 4	1.00 ± 0.04	1.02 ± 0.12	1.07 ± 0.08	1.09 ± 0.07
Nkx2-5	Nkx2.5 Homeobox	1.00 ± 0.04	0.97 ± 0.07	0.92 ± 0.03	0.96 ± 0.02
Miscellaneous					
Slc2a1	Glucose Transporter 1	1.00 ± 0.07	0.88 ± 0.09	0.84 ± 0.07	0.80 ± 0.06
‖Slc2a4	Glucose Transporter 4	1.00 ± 0.05	0.87 ± 0.05	0.69 ± 0.02	0.75 ± 0.05

Total mouse left ventricular RNA was assayed by NanoString technology for the indicated mRNAs and normalized to *Hprt* mRNA levels. Genes marked with "§" and "‖" are known NFATc and MEF2 target genes, respectively. All data (mean ± s.e.m.) are fold-expression compared to the GFP Sham cohort. n = 3 for Sham cohorts; n = 6, 5 for GFP-TAC and PP-GFP -TAC, respectively. † p vs. Sham with same virus; * p vs. GFP-TAC. 2-way ANOVA with matching for each mouse was performed with Tukey post-hoc testing for differences within rows using data before normalization to the GFP Sham cohort.